

Likelihood Models for Forensic Genealogy

William H. Press

Departments of Computer Science and Integrative Biology
The University of Texas at Austin

John Hawkins

Oden Institute of Computational Engineering and Science
The University of Texas at Austin

February 13, 2022

Abstract

In the idealized Morgan model of crossover, we study the probability distributions of shared DNA (identical by descent) between individuals having a wide range of relationships (not just lineal descendants), especially cases for which previous work produces inaccurate results. Using Monte Carlo simulation, we show that a particular, complicated functional form with just one continuous fitted parameter accurately approximates the distributions in all cases tried. Analysis of that functional form shows that it is close to a normal distribution, not in shared fraction f , but in the square-root of f . We describe a multivariate normal model in this variable for use as a practical framework for several general tasks in forensic genealogy that are currently done by less-accurate and less well-founded methods.

1 Introduction

Forensic genealogy seeks the identity of an unknown person (UP) for whom a DNA sample is available, but whose identified genome is not in any database. The UP may be an at-large criminal suspect whose DNA is present at a crime scene [1], or he/she may be an unidentified, deceased victim [2]. Alternatively,

UPs may be adopted individuals seeking to know their biological parents, in which case they are “unknown” in pedigree, not name.

The current methodology of forensic genealogy is to genotype or partially sequence the UP’s DNA using a commercial SNP microarray, and then to upload the file of SNP results in one of several standard formats to a public genome database such as GEDmatch [3]. Remotely on that database, a similarity match against all available genomes is performed, returning a list of genomes that are statistically significant matches to UP, along with identifying information that the owners of those matches have authorized for public release. The similarity score generally reported is the centimorgan length of autosomal matches, exact or near-exact, of the diploid genomes, approximately equivalent to the fraction of autosomal genome that is identical by descent (IBD) [5]. With current public database sizes, it is common that half a dozen or more matches to UPs are reported, with centimorgan scores that may be typical of third or fourth cousins, but closer relatives in favorable cases.

The job of the forensic genealogist is next to construct a probable family tree (or pedigree) from the available match data, and then to place UP convincingly in that tree. Often, matched individuals may not even know that they are mutually related, or exactly how. The genealogist makes use of public records, commonality of names and geographical locations, and other data to hypothesize possible family trees and hypothetical positions for UP in those trees. This conventional, often ingenious, detective work frequently yields more than one seemingly viable hypothesis. Some kind of quantitative calculation of the relative likelihood of the various hypotheses, given the observed centimorgan scores, is thus required.

If fractional genomic matches were deterministic (e.g., if the genomes of third cousins were *exactly* $1/128$ identical by descent), then a probabilistic calculation might be unnecessary. Since, however, the number of crossovers on each chromosome in each meiosis event is stochastic, the centimorgan similarity scores of even fairly close relatives can be intrinsically ambiguous as to what relationship is implied. Current practice is to compare the observed centimorgan scores to distributions derived from the self-reported relationships of users who upload their genomes and link themselves to other uploaded genomes [5]. Each centimorgan score is then assigned a probability for its being at a distance of k meioses, for $k = 1, 2, 3, \dots$, with the probabilities for all k summing to unity. In essence, this is a Bayesian calculation

on the self-reported empirical data with a uniform prior on k . The probabilities for the UP's multiple matches are then most commonly combined by multiplying the individual probabilities as if they were independent [6]. Hypothesized family trees and the location of UP on them can then be assigned relative probabilities proportional to these products, again a kind of Bayes but now with a uniform prior on the hypotheses.

There are various large and small ways that one might improve on the above procedures. That is the subject of this paper. First, one might want to use probability distributions for the fractional IBD match of various familial relationships that come from genetics, not self-reported data. Self-reporting on distant cousin relationships may, for example, be subject to error, as may be the self-reporting of complicated family trees. Second, one might want not to combine distinct relationships into k -meioses classes. For example, the IBD distributions for grandchild and nephew are different, even though their means of $1/4$ shared fraction are the same. (We will show this below.) Third, one might want to take into account that the probabilities for multiple matches to the UP are not independent. For example, if UP's match to individual P is, by chance, higher than average, then UP's match to some Q who is a child of P will also tend to be quite significantly higher than average. (We will make this quantitative below.) Fourth, the priors assumed by the naive methodology can be inconsistent. For example, the uniform prior on k , the meioses distance, may include significant probabilities for values of k that occur in no allowed (by other data) family tree, distorting the results for the allowed family trees.

Sections 2 and 3 of this paper address the first two issues above, as regards the "classical" calculation of the distribution of fraction of shared autosomal genome between related individuals. We will see that previous calculations, in work going back to the 1950s, yield unreliable answers. We will give analytical formulas that, with a small number of fitted parameters (whose values we give), produce accurate estimates. Then, §4 of this paper addresses issues three and four above, that is, how to construct consistent statistical models that can compare whole family trees given multiple measured centimorgan values, accounting for correlations among the measurements.

For mathematical definiteness, we throughout this paper assume a pure Morgan model, in which the probability of a crossover in meiosis is a Poisson random process along the length of each chromosome, with rate 1% probability per centimorgan (by the definition of genetic distance). It is known,

of course, that this is only an approximation, and that the distribution of crossovers is evolutionarily regulated with both signs, that is with both obligate crossover and crossover interference being observed (see, e.g., [7], [8], and references therein). While these are biologically significant effects, we believe the idealizations of genetic distance and random crossover to be adequate for the purposes of this paper, and in any case, given current practice, forward progress for forensic genealogy.

2 Previous Work

2.1 Assuming Poisson Numbers of Common Segments

Although the work of Morgan, famously confirmed experimentally by McClintock and others, could have allowed some estimate of the distribution of fractional shared genome as early as the 1930s, the first such calculations seem to be those of Fisher [9] and Bennett [10] in the 1950s. These authors noted that, for a chromosome of genetic length L (in Morgans), there would be in the mean kL crossover points after k meioses. On the other hand, the fraction of common genome with a specific ancestor must be, on average, 2^{-k} , by symmetry among 2^k ancestors. These facts, plus an assumption that the number of common segments is Poisson distributed, yielded the analytic result

$$p(f|k, L) df = \exp[-kL(2^{-k} + 2f)] kL\sqrt{2^{-k+1}/f} I_1\left(2kL\sqrt{2^{-k+1}f}\right) df \quad (1)$$

where $p(f|k, L)$ is the probability density for a fraction f in common, with $0 < f \leq 1/2$. There is also a massed probability for no commonality ($f = 0$) given by

$$p(0|k, L) = \exp(-k2^{-k}L) \quad (2)$$

This is a striking analytical result, especially the unexpected occurrence of a modified Bessel function I_1 in equation (1). In §6.1 we give a derivation in modern notation, also pointing out where additional assumptions are made. The key question is, how accurate is equation (1)? At the time it was derived, there was no way to know; but it is straightforward now to compare it to exhaustive Monte Carlo computer simulations (described in §6.2). Figure 1 shows results for the conceptually simple case of a single chromosome whose length is the same as the total human genome. Apart from giving the correct

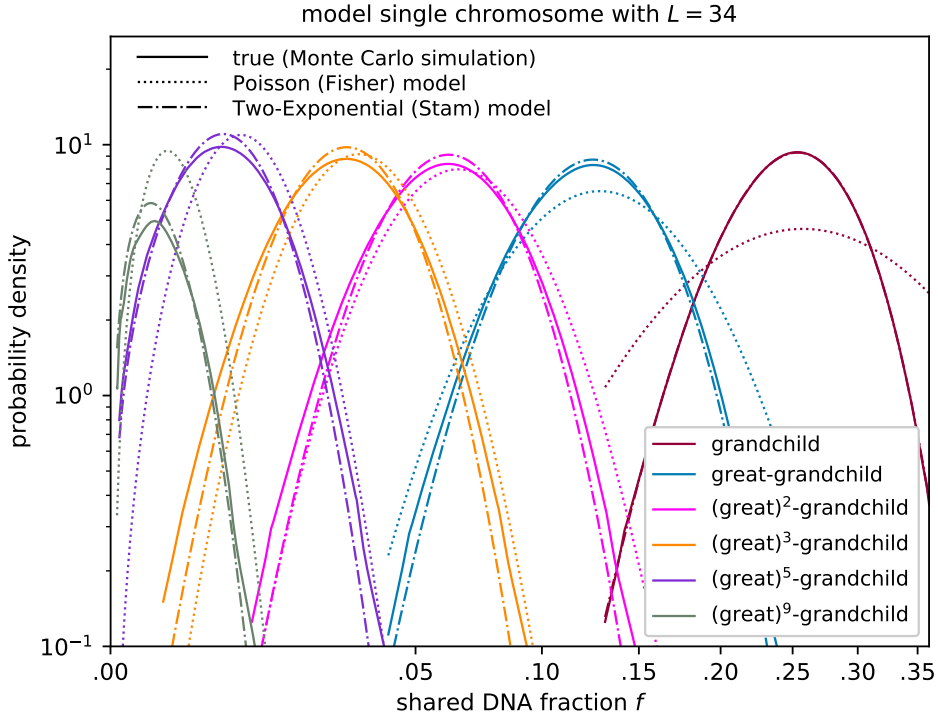


Figure 1: Probability distribution of shared DNA fraction for lineal descendants, in a simplified model with a single chromosome of length 34 Morgans. Solid curves are accurate simulations. Dotted and dash-dot curves are respectively the Poisson and Two-Exponential models (see text). The fraction f is plotted on a square-root distorted scale as explained in §3.2. Probability density is plotted on a logarithmic scale, so that a normal distribution in the scaled abscissa would be exactly an inverted parabola.

mean (by construction), equation (1) agrees poorly with accurate calculation. Its assumptions, which seemed reasonable at the time, turn out to be unjustified. For intuition about how the Poisson model fails, we can note that it positions the starting positions of common segments randomly. In actuality, common segments are self-avoiding, because they are separated by the segments common to other ancestors. Self-avoidance decreases the variance of their number, producing the narrower “true” distributions in Figure 1.

2.2 Assuming Two Exponentials

Understanding the self-avoidance issue, Stam [13], in 1980, modeled two alternating Poisson processes along a chromosome, representing segments in common (state 1), or not in common (state 0), with a specified ancestor. For later use in §3.1, we derive a slight generalization. Suppose that $(p_0, p_1 = 1 - p_0)$ are the probabilities of starting in states $(0, 1)$ at the beginning of the chromosome, and suppose that (λ_0, λ_1) are the rate constants for the two exponentials, so that the segment lengths x are drawn from the exponential probability distributions with densities $p(x|\lambda_i) = \lambda_i \exp(-\lambda_i x)$, for $i = 0, 1$. Then the resulting probability density for the common fraction f , $0 < f < 1$, denoted P^* , can be shown to be

$$\begin{aligned}
 P^*(f|p_0, p_1, \lambda_0, \lambda_1) &= e^{-(1-f)\lambda_0 - f\lambda_1} \\
 &\times \left[\left(\sqrt{(1-f)/f} p_0 + \sqrt{f/(1-f)} p_1 \right) \sqrt{\lambda_0 \lambda_1} I_1 \left(2\sqrt{f(1-f)} \lambda_0 \lambda_1 \right) \right. \\
 &\left. + (\lambda_0 p_0 + \lambda_1 p_1) I_0 \left(2\sqrt{f(1-f)} \lambda_0 \lambda_1 \right) \right]
 \end{aligned} \tag{3}$$

with modified Bessel functions I_0 and I_1 (see §6.3 for derivation). The massed probabilities that the chromosome is entirely in state 0 or 1 are

$$P_i^*(\text{all}|p_0, p_1, \lambda_0, \lambda_1) = p_i \exp(-\lambda_i), \quad i = 0, 1 \tag{4}$$

The normalization is as expected,

$$1 = P_0^*(\text{all}|p_0, p_1, \lambda_0, \lambda_1) + P_1^*(\text{all}|p_0, p_1, \lambda_0, \lambda_1) + \int_0^1 P^*(f|p_0, p_1, \lambda_0, \lambda_1) df \tag{5}$$

In this generalized setting, Stam's [13] results set $p_1 = 2^{-k}$, $p_0 = 1 - 2^{-k}$, $\lambda_1 = kL$, and $\lambda_0 = kL/(2^k - 1)$. This ratio of the λ 's is set by the requirement that the process spend $2^k - 1$ times as long, on average, in state 0 (the $2^k - 1$ ancestors not of interest) as in state 1 (the one ancestor of interest). The result for fractional shared DNA after k meioses is thus expressed in terms of master equation (3) as

$$p(f|k) = 2P^*(2f|1 - 2^{-k}, 2^{-k}, kL/(2^k - 1), kL) \tag{6}$$

with the factor of 2 on f and P^* to renormalize the denominator convention from haploid to diploid chromosome total lengths (e.g., to have grandchild

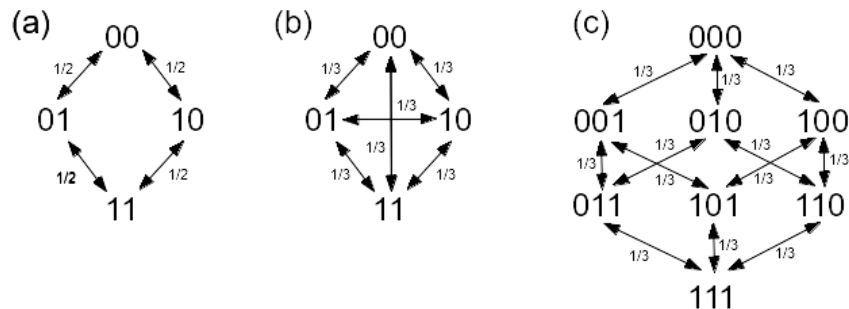


Figure 2: Markov graphs for two and three meioses. (a) Two meioses (actual). (b) Two meioses (two-exponential model). (c) Three meioses (actual). The true return times to a specified ancestor (e.g., 00 or 000) are those associated with hypercube graphs (a) and (c). The two-exponential model approximates the hypercube by the complete graph, e.g., (b).

share $1/4$ with paternal grandparent instead of the equivalent $1/2$ of the paternal haploid).

The dash-dot curves in Figure 1 show the accuracy of the two-exponential model. It is exact for grandchild (explained below, see also [15]), and better than Fisher for other descendants, but not close to exact. In particular, it is seriously in error for relationships that imply small, but nonzero, shared fractions. These are often the relationships most important to forensic genealogists.

2.3 Markov Models

Donnelly [14] first elucidated the precise nature of the failure of the two-exponential model (indeed, any exponential model) to give exact results. (See [16] for more recent references.) Consider the k meioses present in a descendant's chromosome as binary switches with values 0 or 1. One particular setting of these switches, call it the all-zeros value $00\dots 0$, yields DNA in common with a specified ancestor. Each crossover junction on the chromosome flips exactly one switch (changing exactly one zero to one or vice versa). So, along the length of the chromosome, the junctions collectively generate a Markov chain, in particular a random walk on a hypercube graph (see Figure 2).

At each vertex, the distribution of lengths before a transition is $p(x)dx = k \exp(-kx)$, so, in particular, this is the distribution of the individual lengths of common segments, just as in the two-exponential model. However, the distribution of lengths while in the state “*not* 00...0” is not exponential at all. Rather, it is, in any one realization, the sum of $m - 1$ such exponential draws, that is a Gamma distribution of order $m - 1$ where m is itself drawn from the integer distribution of *revisit times* to a vertex under random walks on the hypercube. The two-exponential model in effect substitutes a complete graph like Figure 2(b), whose revisit time is a binomial probability, for the true hypercube Figure 2(a) or 2(c). These coincide only for $k = 1$ (a single meiosis). This is the the grandchild relationship where the two-exponential model was seen in Figure 1 to be exact.

3 Results

The Poisson and two-exponential models are inadequate to our purposes for three reasons. First, they are not accurate enough. Second, they don’t generalize to relationships other than lineal descendants. For example, Figure 3 shows distributions of shared DNA fraction (as determined by Monte Carlo) for a selection of other relationships. One sees (as mentioned above) differences between grandchild and nephew, or great-grandchild and double first cousin, that we need to be able to model. Third, the previous models don’t point us towards the construction of a multivariate model for use when shared DNA fractions to multiple related individuals are known. We now address all three of these issues.

3.1 Fitted Two-Exponential Model

One main result in this paper is a purely empirical (but genetically motivated) fit to distributions such as those shown in Figure 3. We saw that the inaccuracy of Stam’s two-exponential approximation is because, on the hypercube with 2^k vertices, the complement of a single vertex is not the complete graph with $2^k - 1$ vertices. But, we might ask, is there some fictitious number of vertices different from $2^k - 1$ that gives a better approximation? That number need not even be an integer, because the intended use is as a real-valued number in equation (3). As an example, what if we imagine a graph in Figure 2(b) that has not 4 vertices, but 4.414, where the ratio

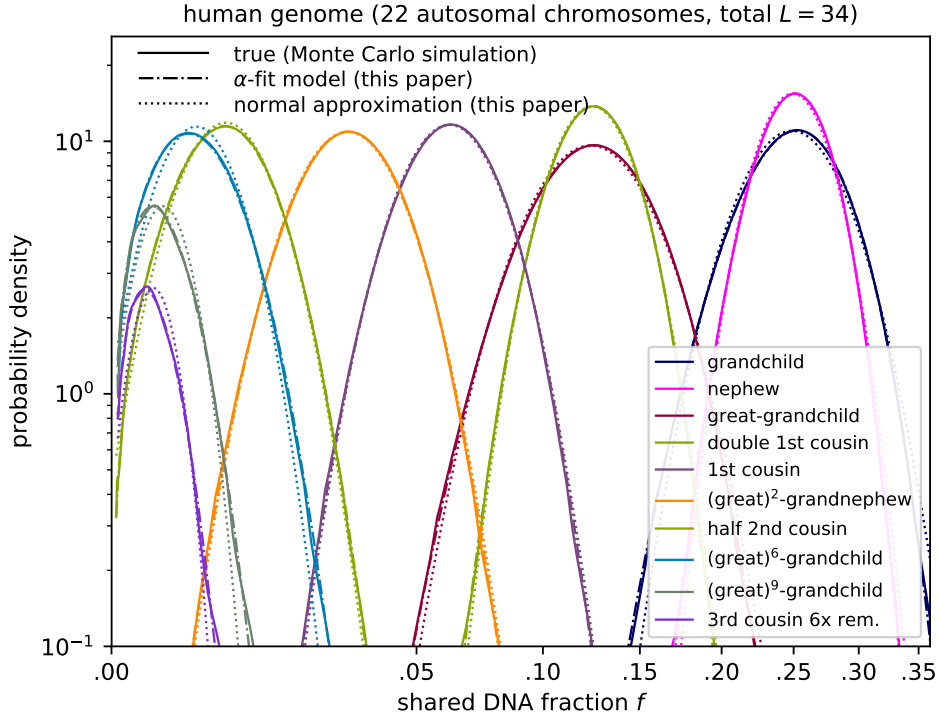


Figure 3: Probability distribution of shared DNA fraction for various relationships. The differences between the accurate Monte Carlo estimates (solid curve) and the model given in this paper (dash-dot curve) are only barely visible in the far tails of the distributions and amount to a few parts in a thousand as measured by Kolmogorov-Smirnov or Kullback-Liebler distances. The dotted curves are the normal approximation to the model in square-root coordinates (see §3.2).

α (here $4.414/4 = 1.104$) is a fitted parameter. Making that change alone would alter the desired mean fractions of 2^{-k} , so we must also scale f to preserve its mean. The specific proposal is to replace equation (6) by the scaled equation

$$p(f|k) = \frac{2}{\alpha} P^* \left[\frac{2f}{\alpha} \mid 1 - \frac{1}{\alpha 2^{k_1}}, \frac{1}{\alpha 2^{k_1}}, \frac{k_2 L}{\alpha 2^{k_1} - 1}, k_2 L \right] \quad (7)$$

(compare to equation 6), where k_1 , k_2 , and α are empirically determined for any particular relationship (e.g., second cousin three times removed) and chromosome or genome length L . The reason for splitting k into the two parameters k_1 and k_2 is that, for relationships other than lineal descendants, the “effective” number of meioses that determine the length of a common segment (k_2) is different from the integer power of two that gives the mean common fraction (k_1). Specifically, the best values for k_2 can be half-integers where changing the state of one switch exposes another that will be right by chance half the time. Section 6.4 works the example for the case of uncle/nephew.

In the following, we fix the value $L = 44$ (Morgans), and compare the result to simulations of the autosomal human genome, 22 chromosomes each having its observed genomic length. One may think of the value 44 as being 34 Morgans (the sum of the genetic lengths of the autosomal chromosomes) plus some fraction of a Morgan for each inter-chromosomal decorrelation; but, in fact, the value is chosen simply empirically as a single value that produces excellent fits to across a wide range of relationships. Our results are not sensitive to the chosen value of L (with correspondingly different values α). We give results for the parameters in equation (7) not only for the case of lineal descendants, but also for other relationships.

We fit for the best value α , by minimizing the Kolmogorov-Smirnov (K-S) distance D_{KS} between equation (7) and the Monte Carlo simulations. D_{KS} is, by definition, the maximum absolute difference between the two cumulative distribution functions at any f . Also of interest (discussion below) is the Kullback-Leibler divergence or relative entropy of the two distributions, denoted D_{KL} . Table 1 gives the values of α obtained, along with D_{KS} and D_{KL} for a representative selection of relationships. The quantity D'_{KL} will be discussed in §3.2 below. Supplemental Table S1 gives results for a much more complete set of relationships, and has accuracy measures comparable to those in Table 1. It is reassuring that the fitted values for α are not too different from 1, implying that the best-fitting fictitious numbers of vertices for the complete graphs are not too different from the actual numbers in the hypercube graphs. (You can get lost in a hypercube—but not too lost.)

The typical accuracies obtained, a few parts in 10^3 , have these interpretations: For D_{KS} , percentile points may be in error by at most that amount, e.g., a 5% critical region might actually be a 4.9% or 5.1% region. For D_{KL} , the actual mean log probability of observed data (per draw) may be parts in

Table 1: Parameters α, k_1, k_2 for the fitted model for representative relationships, and accuracy of the fits.

| | parameters | | | accuracy measures | | |
|-----------------------------------|------------|-------|-------|-------------------|----------|-----------|
| | α | k_1 | k_2 | D_{KS} | D_{KL} | D'_{KL} |
| grandchild | 0.973 | 1 | 1 | 0.0010 | 0.0011 | 0.0051 |
| great-grandchild | 1.036 | 2 | 2 | 0.0016 | 0.0011 | 0.0027 |
| (great) ⁶ -grandchild | 1.380 | 7 | 7 | 0.0027 | 0.0039 | 0.0293 |
| nephew | 1.055 | 1 | 2.5 | 0.0011 | 0.0009 | 0.0029 |
| (great) ² -grandnephew | 1.381 | 4 | 5.5 | 0.0030 | 0.0010 | 0.0014 |
| half-sibling | 1.030 | 1 | 2 | 0.0005 | 0.0009 | 0.0031 |
| half-nephew | 1.018 | 2 | 2.5 | 0.0011 | 0.0009 | 0.0022 |
| 1st cousin | 1.123 | 2 | 4 | 0.0015 | 0.0009 | 0.0016 |
| 1st cousin 3× removed | 1.398 | 5 | 7 | 0.0022 | 0.0005 | 0.0014 |
| double 1st cousin | 1.321 | 1 | 3 | 0.0034 | 0.0011 | 0.0013 |
| half 1st cousin | 1.231 | 3 | 4 | 0.0032 | 0.0011 | 0.0018 |
| half 2nd cousin 2× removed | 1.435 | 7 | 8 | 0.0028 | 0.0052 | 0.0262 |
| 3rd cousin 6× removed | 1.378 | 12 | 14 | 0.0047 | 0.0126 | 0.0724 |

a thousand greater than that indicated by the model. These are negligible errors for the intended application to forensic genealogy. Figure 3, in which the differences are only barely visible as differences between the solid and dashed curves, reinforces this point. Note that the total normalization (area under curve) for the shown example of 3rd cousin 6× removed is less than the other curves. The balance is made up by the massed probability of zero shared DNA for this distant a relationship, as given by equation (4).

Child and sibling are special cases. Child has $f = 1/2$ with massed probability 1, that is, one haploid in each diploid chromosome. Siblings share DNA in both diploid copies. Purely empirically, we find that the parameters

$$p_{\text{sib}}(f)df = P^*(f|0.5, 0.5, 161.5, 161.5)df \quad (8)$$

give an excellent fit with $D_{KS} = 0.0008$. (Roughly speaking, the fact that siblings sum two independent random variables—the two diploid copies—reduces the variance if f , which is well fit by the larger effective value of kL .)

3.2 Normal Approximation

Not immediately apparent in equation (3) is, between the exponential and Bessel function factors, where the peaked distributions seen in Figure 3 actually come from. This becomes clear if we replace the Bessel functions by the two limiting cases of their arguments, either $\gg 1$ or $\ll 1$. We find two possibilities for the leading exponential terms

$$P^*(f) \sim \begin{cases} \exp[-(\sqrt{(1-f)\lambda_0} - \sqrt{f\lambda_1})^2], & \text{or} \\ \exp[-\lambda_0 - (\lambda_1 - \lambda_0)f] \end{cases} \quad (9)$$

As shown in §6.5 below, these are both approximately normal distributions, not in the variable f , but in the variable $s \equiv \sqrt{f}$. Moreover, in the limit $\lambda_0 \ll \lambda_1$ (equation 7 when $2^{k_1} \gg 1$), both forms in equation (9) imply the same variance (in the variable s), $\sigma^2 = 1/(2\lambda_1)$. This explains why the curves in Figure 3 are, by eye, close to parabolic (the normal distributions shown as dotted curves), and why their widths change only slowly as the modal fractions f become small. It is also the reason that we plotted Figures 1 and 3 with a square-root scaled abscissa. We determine the actual parameters (μ, σ) of our normal models not from these asymptotic expansions, but from the Monte Carlo simulations. For intuition about where the square-root coordinate comes from, we can note that square root is the so-called variance stabilizing transformation for the Poisson distribution; so the Poisson approximation in Fisher's model may be making its presence felt.

It would be attractive to use a normal approximation (in coordinate s) to the various distributions, because this would then naturally generalize to a multivariate normal model that can include correlations. Is this accurate enough? One estimate of this the Kullback-Leibler divergence between the normal approximation and the true distribution, written as

$$D'_{KL} \equiv \int_0^1 \log \left(\frac{p(s)}{q(s)} \right) p(s) ds = \langle \log p(s) \rangle - \langle \log q(s) \rangle \quad (10)$$

where angle brackets denote expectation over the true distribution $p(s)ds$, and $q(s)$ denotes the normal approximation. The interpretation is that, for events sampled from the true distribution, D'_{KL} (which is always positive) is, per observation, the mean excess log probability of the observation over that calculated by the normal model. If this were large, then the normal model would, on average, reject plausible observations and would thus not be useful.

However, the quantity D'_{KL} was given, for a selection of relationships, as the last column of Table 1. For all but very distant relationships (e.g., (great)⁶-grandchild or 3rd cousin 6× removed) it is on the order of parts per thousand. This is small enough to make a normal model viable, so we may with some confidence turn to the multivariate case. Figure 3 plotted as dotted curves the normal approximation, visibly less perfect than the fitted two-exponential model, but nevertheless remarkably good.

4 Multivariate Normal Model

Suppose that we have some set T_i , $i = 1, \dots, I$, of hypothesized family trees, and that we are given J measurements f_j , $j = 1, \dots, J$ of the fractional DNA matches between pairs of individuals specified on each tree. We immediately convert to square-root variables by $s_j \equiv \sqrt{f_j}$. Probability densities $p_F(f)df$ and $p_S(s)ds$ are related by the law of transformation of probabilities,

$$p_S(s|i) = 2s p_F(s^2|i) \quad (11)$$

Here the conditioning on i means simply “for the relationship specified for s_j in T_i ”. We denote the normal approximation to $p_S(s|i)$ by $q(s|i)$.

If the measurements s_j were independent, we could write the likelihood of each family tree as

$$L_i = \prod_j p_S(s_j|i) \approx \prod_j q(s_j|i) \quad (12)$$

The Bayes odds comparing two hypotheses (up to a choice of prior, to be discussed in §4.1) would be the ratio of their L_i 's.

We turn to Monte Carlo simulations to see when or whether the assumption of independence might be justified. Table 2 gives values for the correlation coefficient

$$r_{j_1 j_2} = \frac{\langle (s_{j_1} - \langle s_{j_1} \rangle)(s_{j_2} - \langle s_{j_2} \rangle) \rangle}{[\langle (s_{j_1} - \langle s_{j_1} \rangle)^2 \rangle \langle (s_{j_2} - \langle s_{j_2} \rangle)^2 \rangle]^{1/2}} = \frac{\text{cov}(s_{j_1}, s_{j_2})}{\sigma(s_{j_1})\sigma(s_{j_2})} \quad (13)$$

where angle brackets denote the mean of large numbers of trials. Values for a large number of relationship pairs are given systematically in Supplemental Table S2. One finds substantial correlations, especially when, for example,

Table 2: Correlation coefficient for shared DNA fraction for selected pairs of relationships.

| j_1 ($A \leftrightarrow B$) B is A 's: | j_2 ($A \leftrightarrow C$) C is B 's: | $r_{j_1 j_2}$ |
|---|---|---------------|
| sibling | child | 0.76 |
| uncle | child | 0.59 |
| half 3rd cousin | child | 0.74 |
| (many relationships) | child | 0.50–0.77 |
| grandparent | sibling | 0.73 |
| great-great grandparent | sibling | 0.81 |
| sibling | grandchild | 0.40 |
| uncle | grandchild | 0.38 |
| (many relationships) | grandchild | 0.37–0.55 |
| sibling | great-grandchild | 0.27 |

unknown person UP is compared both to a person B and to a sibling, child, or grandchild of B .

A multivariate normal model that includes correlations must utilize the covariance matrix

$$S_{j_1 j_2} \equiv \text{cov}(s_{j_1}, s_{j_2}) = r_{j_1 j_2} \sigma_{j_1} \sigma_{j_2} \quad (14)$$

(with diagonal elements $S_{jj} = \sigma_j^2$). If \mathbf{S}^{-1} denotes the matrix inverse of \mathbf{S} , then one computes from the measured values \hat{s}_j

$$\chi^2 = \sum_{j_1, j_2} (\hat{s}_{j_1} - \langle s_{j_1} \rangle) S_{j_1 j_2}^{-1} (\hat{s}_{j_2} - \langle s_{j_2} \rangle) \quad (15)$$

in terms of which the multivariate normal log likelihood is

$$\log L_i = -\frac{1}{2} \chi^2 - \frac{1}{2} J \log(2\pi) - \frac{1}{2} \log \det \mathbf{S}_i \quad (16)$$

We have appended an index i to \mathbf{S} to underscore the fact that the covariance matrix depends on the hypothesis T_i , not on the measured values $\{\hat{s}_j\}$. Bayes model comparison requires not just the likelihood L_i , but also prior probabilities p_{0i} . We discuss these in the next section.

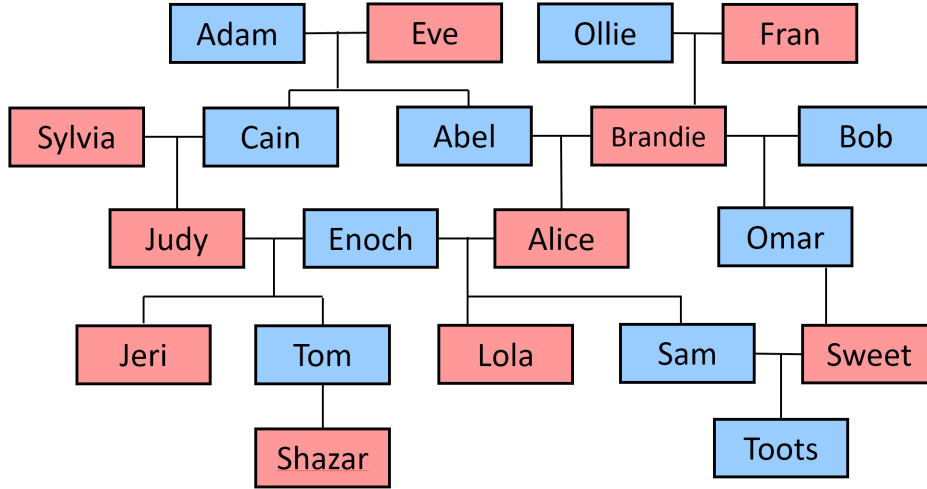


Figure 4: A fictitious, but possible, family tree with endogeny, half- and double-relationships.

4.1 Practical Considerations

The methods developed in this paper have been used to construct a computer code for use by forensic genealogists. We describe here some of the practical issues that arise.

In practice, genealogists cannot be confident that their set of stated hypotheses $\{T_i\}$ include all viable possibilities. In that case, a Bayesian calculation will select the most probable hypothesis, even if that hypothesis is extremely unlikely. This, if undetected, is undesirable. Needed in practice is a rejection criterion for unlikely models, notwithstanding that “rejection” is usually thought of as a frequentist, not Bayesian, concept. If synthetic sets of measured values $\{\hat{s}_j\}$ are drawn from the multivariate normal model of hypothesis T_i , then the values χ^2 (equation 15) will be chi-square distributed with J degrees of freedom. This provides a one-tail rejection criterion for any chosen critical value (tail probability) p_c . In practice, because of various unmodeled effects in the measured data, values of p_c as large as 0.05 or 0.01 may often reject true hypotheses; a value $p_c = 0.001$ is found to be useful.

The Bayes odds (ratio of probabilities) for two hypotheses i_1 and i_2 that

survive rejection is

$$\text{Odds}_{i_1 i_2} = \frac{P_{i_1}}{P_{i_2}} = \frac{L_{i_1}}{L_{i_2}} \times \frac{p_{0i_1}}{p_{0i_2}} \quad (17)$$

where the L_i 's are likelihoods (equation 16), the p_{0i} 's priors. It is well understood in the statistics literature that, in the context of model selection, one cannot simply take $p_{0i} = \text{constant}$ to be the non-informative priors of choice (see, e.g., discussions in [17] and [18]). A part of equation (16) depends on the structure of the model T_i , that is, its number of parameters, J , and the narrowness of their probable ranges, encoded as the value of the determinant $\log \det \mathbf{S}_i$. With constant priors, Bayes favors few parameters with narrow ranges, the so-called *Bayes complexity penalty* or *Ockham factor* [19]. In some applications, this is arguably is a desired feature—but not here. We want to choose priors that will not strongly bias the selection of one hypothesis over another when both are good fits (in the frequentist sense) to the data. Noting that in expectation $\langle \chi^2 \rangle = J$, we choose

$$\log p_{0i} = \frac{1}{2} \log \det \mathbf{S}_i + \frac{1}{2}(1 + \log 2\pi)J_i \quad (18)$$

This depends on the model structure only (not the data), so is legitimate as a prior. Equation (17) now becomes

$$\text{Odds}_{i_1 i_2} = \frac{P_{i_1}}{P_{i_2}} = \exp[-\frac{1}{2}(\chi_{i_1}^2 - \chi_{i_2}^2)] \exp[+\frac{1}{2}(J_{i_1} - J_{i_2})] \quad (19)$$

which has the desired property. Almost always we will have $J_{i_1} = J_{i_2}$, in which case equation (19) involves only the χ^2 's.

If the T_i 's are a complete set of (non-negligible) hypotheses, as required by Bayes Theorem, then their absolute individual probabilities are

$$P(T_i | \{\hat{s}_j\}) = \frac{\text{Odds}_{ik}}{\sum_i \text{Odds}_{ik}} \quad (20)$$

which is numerically the same for any choice of T_k against which to measure.

Although the Supplemental Material includes the extension of Tables 1 and 2 to many relationships (and, for correlation, many pairs of relationships), it is not practical to catalog all possible relationships that may arise. Family situations that ultimately give rise to forensic work are often complicated. As a fictitious, but possible, example, Figure 4 shows a family tree with endogeny (inbreeding), half, and double relationships. In the figure,

Shazar and Toots are simultaneously third cousins and half first cousins. Lola is Toots' aunt by descent from Adam and Eve, but Lola and Toots are also both also descended from Ollie and Fran in a complicated way, through half-siblings Alice and Omar. A practical code must therefore have the capability of doing new simulations, capturing the parameters of the multivariate normal model, that is, the means $\langle s_j \rangle$ and covariances $\text{cov}(s_{j_1}, s_{j_2})$. Our simulation is described below in §6.2.

One might ask: If we are going to do simulations anyway, then why do we need a model (and the whole apparatus of this paper) anyway? The answer is that, in the multivariate case of $J > 1$, there is no simple or generally accepted model-independent way to estimate the likelihoods L_i from the simulation data. Even with many trials, a simulation does not densely populate the J -dimensional space of measured values. A model simultaneously estimates the local density and interpolates among scattered points in high-dimensional space.

5 Discussion

Using a Monte Carlo simulation (§6.2), we studied the probability distributions of fractional common DNA between human individuals related in various ways—not just lineal descendants. We showed why previous analytic attempts at calculating these distributions produced inaccurate results. We then showed that a particular functional form, defined by equations (3) and (7) with essentially a single continuous fitted parameter, reproduces the simulation data with accuracy of parts per thousand (measured in multiple ways) over a wide range of complex relationships.

Analysis of that functional form, showed that it in turn can be well approximated by a normal distribution, not in shared DNA fraction f , but rather in \sqrt{f} . That led us to propose a multivariate normal model in \sqrt{f} as a general framework for use in forensic genealogy, one that evaluates the respective likelihoods of different hypothesized family trees, given a set of shared DNA measurements. We gave a detailed description of that model in §4. These ideas are being used in a code that we are developing in cooperation with, and for use by, practicing forensic genealogists.

Centimorgan values for shared DNA as reported by genome database organizations such as GEDmatch [3] are in no sense exact. Not only are se-

quencing or other errors possible in the uploaded data, but there are also algorithmic choices in the match calculation that are not visible to the database user. For this reason, and also because the Morgan crossover model is itself not exact, it is found useful to add a small constant measurement-error term ϵ^2 to the diagonal elements of the covariance matrix \mathbf{S} (equation 14). In the absence of other information, the constant $\epsilon = 0.03$ seems to work well, but the value should be adjustable by the user. In any particular instance, ϵ can be adjusted to make known-true family trees give reasonable χ^2 probabilities. Since ϵ^2 is added to \mathbf{S} in square-root coordinates, its centimorgan equivalent varies with measured value. For a constant $\epsilon = 0.03$ the implied error is about ± 35 at 100 centimorgans, rising to about ± 100 at 1000 centimorgans.

6 Methods and Materials

6.1 Poisson Model of Fisher and Bennett

Fisher [9] and Bennett [10] argued as follows: After k meioses of a haploid chromosome of length L (in Morgans), the mean length in common with any one ancestor is $2^{-k}L$. Further, there are then on average kL junction points from one or another of the meioses, distributed uniformly randomly. An IBD segment from any one ancestor terminates when it encounters any one such junction, so its length is exponentially distributed, $p(x)dx = k \exp(-kx)dx$. Thus, for any specific number n of such segments in common, their total length x is the sum of n such exponential deviates. Such a sum is Gamma(n, k) distributed. We *assume* negligible correlation between the mean number of common segments \bar{n} and their mean length $1/k$. The intuition for this is that the events that start a segment (responsible for their number) are different from the events that terminate a segment (responsible for their lengths). The total length is then the product of the mean number and mean length, implying

$$\bar{n} = k2^{-k}L \tag{21}$$

Now further *assume* that the actual number n of common segments is Poisson distributed around its mean because (intuitively) the separated segments occur independently of each other. Then the distribution of total

common length x is

$$\begin{aligned} p(x|k, \bar{n})dx &= \sum_{n=1}^{\infty} \text{Gamma}(x|n, k) \text{Poi}(n|\bar{n})dx \\ &= \exp(-\bar{n} - kx) \sqrt{k\bar{n}/x} I_1(2\sqrt{k\bar{n}x})dx \end{aligned} \quad (22)$$

where $\text{Poi}(k|\lambda)$ and $\text{Gamma}(x|n, \lambda)$ denote the Poisson and Gamma distribution densities,

$$\text{Poi}(k|\lambda) = \frac{\lambda^k}{k!} \exp(-\lambda), \quad \text{Gamma}(x|n, \lambda) = \frac{\lambda^n x^{n-1}}{(n-1)!} \exp(-\lambda x) \quad (23)$$

Remarkably, the sum yielding a modified Bessel function I_1 can be done by Mathematica. The missing term in the sum, $n = 0$, is the massed probability of having no common segments, $p_0 = \text{Poi}(0|\bar{n})$.

Transforming the result from the variable x to the shared DNA fraction $f = x/(2L)$ gives the probability density for f in the range $0 < f \leq 1/2$,

$$p(f|k, L) df = \exp[-kL(2^{-k} + 2f)] kL \sqrt{2^{-k+1}/f} I_1\left(2kL \sqrt{2^{-k+1}f}\right) df \quad (24)$$

The reason for the factor $1/2$ in the definition of f is that f is here defined as the fraction of total genome, including two diploid chromosomes, one of which comes from an unrelated parent. For the same reason, we have $p(f|k, L) = 0$ for $1/2 < f < 1$. The massed probability at $f = 0$ is

$$p(0|k, L) = \exp(-k2^{-k}L) \quad (25)$$

Equation (1) has the desired probability normalization,

$$1 = p(0|k, L) + \int_{f=0}^1 p(f|k, L) df \quad (26)$$

The case $k = 1$ corresponds to the relation of grandparent to grandchild (separated by a single meiosis in the intervening parent); $k = 2$ corresponds to great-grandchild, etc.

Figure 1 showed that the above argument, while seductive, does not produce accurate results.

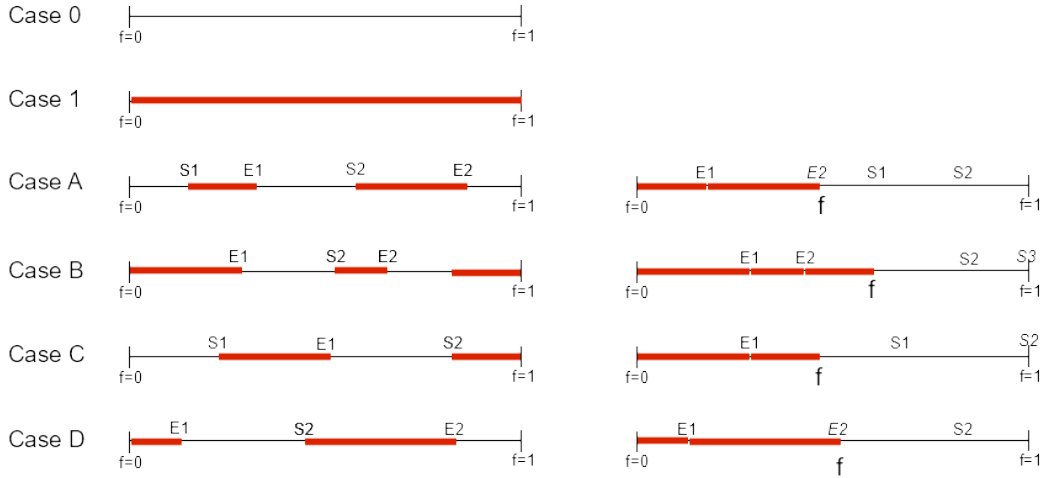


Figure 5: Cases for computing the probability of obtaining a total fraction f for one of two alternating Poisson processes, states 0 and 1. State 1 segments are denoted as thicker red lines. In the right-hand column these have been grouped to the left, showing their total fraction f . See text for details.

6.2 Computer Simulation

We take the total genetic length of the haploid human genome to be 3400 centimorgans, divided among 22 chromosomes in proportion to the empirical lengths published by Family Tree DNA [11, 12]. We discretize in segments of 0.1 centimorgan, each thus having independent probability 0.001 of being a crossover location. For a single trial, full diploid genomes of every individual at the “top” of a given family tree (that is, not the result of a mating within the tree) are initialized with an identifier unique to that individual. Descendant genomes are then filled in by simulating random crossovers, copying the unique identifier that is inherited by descent. For all pairs of interest, a value for the IBD common fraction is summed by direct comparison and saved as one draw from the desired distribution. Trials are repeated typically 10^5 – 10^6 times to populate the distribution.

6.3 Derivation of Equation (3), the Two-Exponential Model

Although the general idea is implicit in [13], we give here a streamlined and slightly generalized derivation. There are six disjoint possibilities to consider. We denote them by (0,1,A,B,C,D), as shown in Figure 5. Cases 0 and 1 represent the massed probability of staying in state 0 or 1 for the entire length. The respective probabilities are

$$P_i^*(\text{all} | p_0, p_1, \lambda_0, \lambda_1) = p_i \text{Poi}(0, \lambda_i) = p_i \exp(-\lambda_i), \quad i = 0, 1 \quad (27)$$

where $\text{Poi}(j, \lambda)$ denotes the probability of drawing j from a Poisson distribution with mean λ .

Cases A, B, C, and D, represent the four possibilities of starting and/or ending in states 0 or 1. The figure shows the correspondence. Red segments are state 1, with start and end positions denoted by S_k and E_k . For each of A,B,C,D, we can imagine regrouping all the segments in state 1 to the left, all in state 0 to the right, as shown in the right column of the figure. The dividing line is the fraction f of the length in state 1. Now notice that every S_k and E_k is either an ‘‘interior’’ junction, which can be anywhere in its respective state, or a ‘‘pinned’’ junction that is located exactly at f (state 1) or $1-f$ (state 0). This is enough to immediately write the probability that f lies between f and $f + df$ in the four disjoint cases as the product of a starting probability (p_0 or p_1), two interior Poisson probabilities for the observed numbers of interior junctions, and a pinned probability ($\lambda_0 df$ or $\lambda_1 df$), of course summed over all possible numbers of segments:

$$\begin{aligned} P(f \cap A)df &= p_0 \sum_{i=1}^{\infty} \text{Poi}(i-1 | f\lambda_1) \text{Poi}(i | (1-f)\lambda_0) (\lambda_1 df) \\ P(f \cap B)df &= p_1 \sum_{i=1}^{\infty} \text{Poi}(i | f\lambda_1) \text{Poi}(i-1 | (1-f)\lambda_0) (\lambda_0 df) \\ P(f \cap C)df &= p_0 \sum_{i=0}^{\infty} \text{Poi}(i | f\lambda_1) \text{Poi}(i | (1-f)\lambda_0) (\lambda_0 df) \\ P(f \cap D)df &= p_1 \sum_{i=0}^{\infty} \text{Poi}(i | f\lambda_1) \text{Poi}(i | (1-f)\lambda_0) (\lambda_1 df) \end{aligned} \quad (28)$$

The sums can all be done analytically (in Mathematica), giving the disjoint

probabilities

$$\begin{aligned}
P(f \cap A)df &= p_0 e^{-(1-f)\lambda_0 - f\lambda_1} \sqrt{(1-f)/f} \sqrt{\lambda_0 \lambda_1} I_1 \left(2\sqrt{f(1-f)\lambda_0 \lambda_1} \right) \\
P(f \cap B)df &= p_1 e^{-(1-f)\lambda_0 - f\lambda_1} \sqrt{f/(1-f)} \sqrt{\lambda_0 \lambda_1} I_1 \left(2\sqrt{f(1-f)\lambda_0 \lambda_1} \right) \\
P(f \cap C)df &= p_0 e^{-(1-f)\lambda_0 - f\lambda_1} \lambda_0 I_0 \left(2\sqrt{f(1-f)\lambda_0 \lambda_1} \right) \\
P(f \cap D)df &= p_1 e^{-(1-f)\lambda_0 - f\lambda_1} \lambda_1 I_0 \left(2\sqrt{f(1-f)\lambda_0 \lambda_1} \right)
\end{aligned} \tag{29}$$

The sum of the four cases gives equation (3).

6.4 Uncle/Nephew Is Best Fit by Half-Integral Number of Meioses

In Table 1, for the relationships nephew or half-nephew and descendants, recommended values for the parameter k_2 are half-integral. We here give a heuristic explanation, with the case of uncle/nephew as an example. We denote the relevant individuals and one of their diploid chromosomes as follows: Grandpa (A)(A'), Grandma (B)(B'); their two children Uncle (A, A')(B, B') and Father (A, A')(B, B'); an exogamous Mother (\cdot)(\cdot); and Nephew, the son of Father and Mother (A, A', B, B')(\cdot). We refer to the diploid chromosomes in the order given as “left” and “right”.

At a particular location on the chromosome of interest, there are five relevant “switches” with values 0 or 1: 1. Is Nephew’s left an (A, A') (0) or a (B, B') (1)? 2. Is Uncle’s left an A (0) or an A' (1)? 3. Is Father’s left an A (0) or an A' (1)? 4. Is Uncle’s right a B (0) or a B' (1)? 5. Is Father’s right a B (0) or a B' (1)? Four patterns of these switches (in the order 1 to 5) produce a match between Nephew and Uncle: 000 $\cdot\cdot$, 011 $\cdot\cdot$, 1 $\cdot\cdot$ 00, 1 $\cdot\cdot$ 11. Here “dot” means either value, 0 or 1. Four other patterns produce no match: 001 $\cdot\cdot$, 010 $\cdot\cdot$, 1 $\cdot\cdot$ 01, and 1 $\cdot\cdot$ 10. These eight patterns exhaust all possibilities. Since half of them produce a match, we must have $k_1 = 1$ in equation (7).

Now for k_2 , consider just the three “active” switches in each of the eight patterns, i.e., those not denoted by a dot. If changing any one switch terminated a match between Nephew and Uncle, then we would have $k_2 = 3$, by the argument in §2.3. But, here, if we change the first switch, then the

dots change positions (from 2-3 to 4-5 or vice versa), exposing two different non-dotted positions. Half the time, the cases 00 or 11, the newly exposed positions will happen to continue a match. So switch number 1 is really only half a switch and the heuristic trial value is $k_2 = 2.5$. The validation is that with this value and a fitted value for α , equation (7) gives an excellent fit, as seen in Figure 3.

6.5 Asymptotic Forms Suggest Square-Root Fraction Coordinate

The argument of both Bessel functions in equation (3) is

$$\eta = 2\sqrt{f(1-f)\lambda_0\lambda_1} \quad (30)$$

For $\eta \gg 1$,

$$I_0(\eta) \approx I_1(\eta) \approx \frac{1}{\sqrt{2\pi\eta}} \exp(\eta) \quad (31)$$

and equation (3) can be written

$$P^*(f) = (\text{sub-exponential factors}) \times \exp[-(\sqrt{(1-f)\lambda_0} - \sqrt{f\lambda_1})^2] \quad (32)$$

Since we are generally interested in $f \ll 1/2$, equation (32) is suggestive of a normal distribution in the coordinate $s \equiv \sqrt{f}$. One easily calculates that the maximum exponential argument occurs at $s_{\max} = \sqrt{\lambda_0}/(\sqrt{\lambda_0} + \sqrt{\lambda_1})$ and that the second derivative there implies a variance,

$$\sigma^2 = \frac{1}{2} \frac{\lambda_1}{(\lambda_0 + \lambda_1)^2} \approx \frac{1}{2} \frac{1}{\lambda_1} \quad (33)$$

where the last approximation is for $\lambda_0 \ll \lambda_1$ (compare equations 6 and 7). For the opposite asymptotic limit $\eta \ll 1$, we have $I_0(\eta) \approx 1$ and $I_1(\eta) \approx \frac{1}{2}\eta$. Now

$$P^*(f) = (\text{sub-exponential factors}) \times \exp[-\lambda_0 - (\lambda_1 - \lambda_0)s^2] \quad (34)$$

implying a normal distribution in s with mean zero and

$$\sigma^2 = \frac{1}{2} \frac{1}{(\lambda_1 - \lambda_0)} \approx \frac{1}{2} \frac{1}{\lambda_1} \quad (35)$$

The fact that both asymptotic limits give (for $\lambda_0 \ll \lambda_1$) the same variance in the s -coordinate, even as the means go to zero, explains the utility of the square-root distorted scale in Figures 1 and 3.

Acknowledgments

We have benefitted from discussions with Margaret Press and Colleen Fitzpatrick, founders of the DNA Doe Project [20].

References

- [1] Kolata, Gina, and Murphy, Heather, “The Golden State Killer Is Tracked Through a Thicket of DNA, and Experts Shudder,” *New York Times*, April 27, 2018, at <https://www.nytimes.com/2018/04/27/health/dna-privacy-golden-state-killer-genealogy.html>.
- [2] Zhang, Sara, “An Abandoned Baby’s DNA Condemns His Mother,” *The Atlantic*, March 13, 2019, at <https://www.theatlantic.com/science/archive/2019/03/38-years-later-dna-leads-to-teenager-who-abandoned-her-baby-in-a-ditch/584683/>
- [3] GEDmatch.com, information at <https://www.gedmatch.com/tos.htm>
- [4] Fisher, R.A., *The Theory of Inbreeding* (Edinburgh: Oliver and Boyd, 1949).
- [5] Catherina A. Ball, Mathew J. Barber, et al. “AncestryDNA Matching White Paper” (March 31, 2016 update) at <https://www.ancestry.com/dna/resource/whitePaper/AncestryDNA-Matching-White-Paper.pdf>
- [6] Leah Larkin, “Science the Heck out of Your DNA”, Part 7, at <https://thednageek.com/science-the-heck-out-of-your-dna-part-7/>
- [7] Jones, G.H., and Franklin, F.C.H. “Meiotic Crossing-over: Obligation and Interference,” *Cell*, **126**, 246-248 (2006).
- [8] Mezard, C., Jahns, M.T., and Grelon, M. “Where to cross? New insights into the location of meiotic crossovers,” *Trends in Genetics*, **31**, 394-401 (2015).
- [9] Fisher, R.A., “A fuller theory of ‘junctions’ in inbreeding,” *Heredity*, **8**, 187-197 (1954).

- [10] Bennett, J.H., “Junctions in inbreeding,” *Genetica*, **26**, 392-406 (1953).
- [11] “Family Tree DNA” at <https://www.familytreedna.com>
- [12] ISOGG Wiki, “centiMorgan”, at <https://isogg.org/wiki/CentiMorgan> .
- [13] Stam, P. “The distribution of the fraction of the genome identical by descent in finite random mating populations,” *Genet. Res. Camb*, **35**, 131-155 (1980).
- [14] Donnelly, K.P., “The probability that related individuals share some section of genome identical by descent,” *Theoretical Population Biology*, **23**, 34-63 (1983).
- [15] Walters, K., and Cannings, C. “The probability density of the total IBD length over a single autosome in unilineal relationships,” *Theoretical Population Biology*, **68**, 55-63 (2005).
- [16] Tiret, M., and Hospital, F. “Blocks of chromosomes identical by descent in a population: Models and predictions,” *PLOS One*, (12) 11: e0187416 (2017).
- [17] Berger, J.O., and Pericchi, L.R., “The Intrinsic Bayes Factor for Model Selection and Prediction,” *J. Am. Statistical Assoc.*, **91**, 109-122 (1996).
- [18] Wasserman, L., “Bayesian Model Selection and Model Averaging,” *J. Math. Psychology*, **44**, 92-107 (2000).
- [19] P.C. Gregory and T.J. Lored, in *Maximum Entropy and Bayesian Methods: Seattle, 1991* (C.R. Smith, G.J. Erickson, and P.O. Neudorfer, eds.), Springer (1991), p. 90.
- [20] “DNA Doe Project” at <http://dnadoeproject.org/> .

Supplemental Materials

The Supplemental Materials can be found on GitHub at <https://github.com/whpress/forensicgenealogy> and consist of computer files, some large, as follows:

- File *SupplementalTable1.tsv* (7KB) Values k_1 , k_2 , α , D_{KS} , D_{KL} , D'_{KL} for the fitted models of 96 relationships in the files *dependsdata_*_23.txt*. Table 1 in the main text gave a representative selection.
- File *SupplementalTable2.xlsx* (17 KB): Coefficients of correlation r for 173 pairs of relationships drawn from *bigrun_data.out*, above. Table 2 in the main text gave a representative selection.
- Files *dependsdata_*_23.txt* (each about 50 MB): Centimorgans of common DNA for one million Monte Carlo simulations of the relationships (and also descendants ≤ 9 times removed) for lineal descendant, 1st cousin, 2nd cousin, 3rd cousin, double 1st cousin, nephew, half 1st cousin, half 2nd cousin, half third cousin, and half nephew.
- File *bigrun_data.out* (470 MB): Centimorgans of common DNA for one million Monte Carlo simulations among all pairs of descendants to five generations of siblings and half-siblings. Stored as zip file broken into two pieces. Can be reconstituted with 7-zip (e.g.).